

REFERENCE-BASED TRELLIS CODED MODULATION SCHEMES FOR SHADOWED RICIAN FADING CHANNELS

C. Tellambura, V. K. Bhargava, Fellow IEEE,
 Department of Electrical & Computer Engineering,
 University of Victoria P.O. Box 3055,
 Victoria B.C., Canada V8W 3P6
 tel(604) 721-6043, email: chintha@sirius.uvic.ca.

Abstract—The Canadian mobile satellite (MSAT) channel has been modelled as the sum of lognormal and Rayleigh components to represent foliage attenuation and multipath fading, respectively. Several authors have applied trellis coded modulation (TCM) schemes to this channel, estimating the bit error performance via computer simulation. In this paper, a general expression is presented for the pairwise error probability (PEP) of TCM schemes transmitted over this channel under ideal interleaving. The expression can be specialized to several cases including ideal coherent detection, pilot-tone aided detection, and differential detection. The results are substantiated by means of computer simulation.

I. INTRODUCTION

To improve the performance of mobile communication systems (e.g., mobile satellite and cellular mobile systems), several authors have considered the application of TCM schemes to such channels. Typically, mobile satellite channels are modelled as Rician; that is, the received signal consists of a *constant* line of sight (LOS) signal component and a Rayleigh distributed diffuse signal component. In contrast, to account for the effect of foliage attenuation or blocking in a shadowed channel, the LOS component is assumed to be distributed as a lognormal variate. In application to the Canadian MSAT program, this model has been found to agree with measured data. A lower angle of elevation ($15^\circ - 20^\circ$) between a mobile user and a geosynchronous satellite implies that the effect of shadowing is more pronounced in Canada than in the United States [1]. We shall describe this model in more detail later.

Many studies have been carried out to determine the applicability of TCM to this channel model; some of them include [1, 2, 3]. In general they use computer simulation to predict error performance. Thus, unlike the case of Rician fading channels, an analytical basis for evaluating the performance of TCM over the shadowed Rician channel is missing. This paper attempts to fill the gap by providing new, analytical error bounds for TCM schemes over shadowed Rician channels. The error bounds can be applied for reference-based coding systems such as coherently differential detection, pilot-tone based detection, and pilot-symbol aided detection. The resulting bounds resemble those of the Rician channel, and as such can be used for both evaluating the bit error performance and for finding optimal codes for such channels.

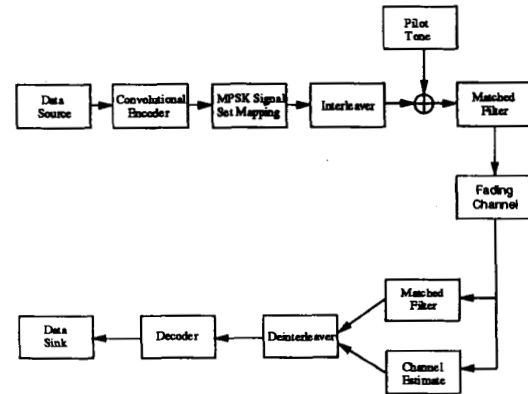


Figure 1: System Model.

In [4], the authors derive the approximate PEP of both TC-MPSK (trellis coded M-ary phase shift keying) and TC-MDPSK (trellis-coded M-ary differential phase shift keying) over Rician, ideally interleaved channels. In this paper, we extend this earlier result to the shadowed Rician fading channel. The accuracy of the resulting bounds is confirmed by Monte-Carlo simulation results.

II. SYSTEM AND CHANNEL MODEL

We consider a typical system model as shown in Fig. 1. Binary input data is convolutionally encoded at rate $n/(n+1)$. The encoded $n+1$ bit words are block interleaved and mapped into a sequence $\mathbf{x} = (x_1, x_2, \dots, x_N)$ of M-ary PSK symbols, which constitute a normalized constellation, that is, $|x_k|^2 = 1$ for all symbols. The receiver deinterleaves and then applies soft-decision Viterbi decoding.

In this work, we assume *ideally interleaved* channels. The ensuing independent fading approximation allows us to obtain a simple upper bound on the average bit error probability, which gives the performance limits of practical systems. In accordance with this assumption, we ignore the scrambling of the encoder output sequence by the interleaver. Thus, the transmitted signal is represented in the baseband as [5]

$$e(t) = \sum_{k=-\infty}^{\infty} v_k s(t - kT_s) \quad (1)$$

parameter	Light	Average	Heavy
b_0	0.158	0.126	0.0631
μ_0	0.115	-0.115	-3.91
$\sqrt{d_0}$	0.115	0.161	0.806

Table 1. Shadowed Rician Parameters.

where $s(t)$ is a unit-energy pulse such that it satisfies Nyquist's conditions for zero inter-symbol interference after the receiving filter, and v_k denotes the k -th transmitted symbol. The receiver employs a filter matched to $s(t)$. Therefore, the received sample corresponding to the k -th coded symbol can be denoted by

$$y_k = \alpha_k v_k + n_k \quad (2)$$

where n_k is a complex-Gaussian random variable with zero mean and variance $\sigma^2 = (2\gamma_s)^{-1}$ where $\gamma_s = \bar{E}_s/N_0$. Here \bar{E}_s denotes the average signal energy, and N_0 is the single-sided noise spectral density of the additive noise.

For the shadowed Rician channel model, α_k is the sum of three components:

$$\alpha_k = A_k + \xi_k + j\eta_k \quad (3)$$

where both ξ_k and η_k are two real independent Gaussian random variables with zero mean and variance b_0 . The remaining term A_k is equal to $\exp(\zeta_k)$ where ζ_k is Gaussian with mean μ_0 and variance d_0 (note that A_k is a constant for non-shadowed Rician fading channels.). The measured parameters of this model are given in Table 1 [1].

As defined in (3), A_k is a lognormally distributed random variable having the probability density function

$$p(x) = \begin{cases} \frac{1}{\sqrt{2\pi d_0 x}} \exp\left(-\frac{(\log(x) - \mu_0)^2}{2d_0}\right), & x > 0 \\ 0, & \text{elsewhere.} \end{cases} \quad (4)$$

III. ANALYSIS

For a sequence of true channel gains $(\alpha_1, \alpha_2, \dots, \alpha_N)$, there corresponds a sequence of channel estimator [5] outputs denoted as $(\hat{\alpha}_1, \hat{\alpha}_2, \dots, \hat{\alpha}_N)$. Obviously, the performance of the coded system will be heavily dependent upon the accuracy of these estimates. As in [5], we take the Viterbi decoder metric to be Euclidean; namely,

$$m(y_k, x_k) = -|y_k - \beta \hat{\alpha}_k x_k|^2 \quad (5)$$

where β is equal to $\mu \sqrt{b_0/b_1}$. Also, the variance of $\hat{\alpha}_k$ is $b_1 = \frac{1}{2}(\hat{\alpha}_k - \bar{\alpha}_k)(\hat{\alpha}_k - \bar{\alpha}_k)^*$ where $*$ denotes the complex conjugate. The normalized correlation coefficient between $\hat{\alpha}_k$ and α_k is $\mu = \frac{1}{2}(\alpha_k - \bar{\alpha}_k)(\hat{\alpha}_k - \bar{\alpha}_k)^*/\sqrt{b_0 b_1}$.

The PEP $P(\mathbf{x} \rightarrow \hat{\mathbf{x}})$ is the probability of choosing the codeword $\hat{\mathbf{x}} = (\hat{x}_1, \hat{x}_2, \dots, \hat{x}_N)$ when $\mathbf{x} = (x_1, x_2, \dots, x_N)$ was transmitted, given \mathbf{x} and $\hat{\mathbf{x}}$ are the only choices. Assign the set of subscripts k_i , ($i = 1, 2, \dots, L$), arranged in ascending order, for which $x_{k_i} \neq \hat{x}_{k_i}$. Note that L is the Hamming distance between \mathbf{x} and $\hat{\mathbf{x}}$. The smallest possible L , L_{min} , is known as the code diversity. The PEP, by using the fact that the total metric for a codeword is the sum of component metrics, is

$$P(\mathbf{x} \rightarrow \hat{\mathbf{x}}) = \Pr\left\{\sum_{i=1}^L \text{Re}\left[y_{k_i} \beta^* \hat{\alpha}_{k_i}^* (x_{k_i} - \hat{x}_{k_i})^*\right] < 0\right\}. \quad (6)$$

For the PEP in (6), under the conditions $\gamma_s \rightarrow \infty$, and $\mu \approx 1$, an approximation has been derived in [4, Eq. (30)]. As shown there, for the Rician fading channel we have

$$P(\mathbf{x} \rightarrow \hat{\mathbf{x}}) \cong B(L) \prod_{i=1}^L \frac{\Gamma \exp\left(\frac{A^2 \theta d_i^2}{b_0 |\mu|^2 d_i^2 + \Gamma}\right)}{b_0 |\mu|^2 d_i^2 + \Gamma} \quad (7)$$

where $d_i^2 = |x_{k_i} - \hat{x}_{k_i}|^2$,

$$B(L) \cong \frac{1}{\sqrt{2\pi(2L+1)}}, \Gamma = 4((1-|\mu|^2)b_0 + \sigma^2), \quad (8)$$

and

$$\theta = \left[-\beta + \frac{2(b_0 + b_1 + \sigma^2)|\beta|^2 - 4\beta|\mu|^2 b_0}{\Gamma}\right]. \quad (9)$$

In the following, we assume that the lognormal component varies slowly in comparison to the multipath component. Consequently, the lognormal variate A_k in (3) will remain constant during short error events. In other words, the interleaving depth is sufficient to break up correlations due to multipath components but not those due to the shadowing component.

The PEP here is obtained by averaging the above with respect to the pdf of A :

$$P(\mathbf{x} \rightarrow \hat{\mathbf{x}}) \cong \int_{-\infty}^{\infty} \left[B(L) \prod_{i=1}^L \frac{\Gamma \exp\left(\frac{A^2 \theta d_i^2}{b_0 |\mu|^2 d_i^2 + \Gamma}\right)}{b_0 |\mu|^2 d_i^2 + \Gamma} \right] p(A) dA \quad (10)$$

where $p(A)$ is given by (4). For light and average shadowed Rician cases (where d_0 is small), each of these integrals can be obtained by an approximation given in [6, Eq. (53)]. Consequently, we maintain that for the light and average shadowing models the PEP is given by

$$P(\mathbf{x} \rightarrow \hat{\mathbf{x}}) \cong B(L) \left(\prod_{i=1}^L \frac{\Gamma \exp(-c_i \varrho^2)}{b_0 |\mu|^2 d_i^2 + \Gamma} \right) C \quad (11)$$

where $\varrho = \exp(\mu_0)$,

$$c_i = \frac{-\theta d_i^2}{b_0 |\mu|^2 d_i^2 + \Gamma}, \quad (12)$$

$c_0 = \sum_{i=1}^L c_i$, and $C = (1 + 2d_0 c_0 \varrho^2 [c_0 \varrho^2 - 1])$. Unfortunately, this expression cannot be used with the transfer function method because c_0 consists of additive terms, a manifestation of our slow fading assumption. As in [6], we compute c_0 only for the shortest error event, and incorporate this value of c_0 into $B(L)$. Thus, for this case

$$B(L) = \frac{1}{\sqrt{2\pi(2L+1)}} (1 + 2d_0 c_0 \varrho^2 [c_0 \varrho^2 - 1])_{L_{min}} \quad (13)$$

A. IDEAL TC-MPSK

In this case, we have an ideal estimate of the channel gain; that is, $\hat{\alpha}_k = \alpha_k$. Thus $b_1 = b_0$, $\mu = 1$, $\beta = 1$, and $\theta = -0.5$. Substituting these values in (11) leads to the expression

$$P(\mathbf{x} \rightarrow \hat{\mathbf{x}}) \cong B_1(L) \prod_{i=1}^L \frac{\exp(-c_i \varrho^2)}{1 + \frac{b_0}{2} |x_{k_i} - \hat{x}_{k_i}|^2 \gamma_s}. \quad (14)$$

Furthermore, the constant c_0 is given by

$$c_0 \approx \frac{0.5L_{\min}}{b_0}, \quad \gamma_s \rightarrow \infty, \quad (15)$$

which is independent of the distance structure of the shortest error event. Thus, $B(L)$ depends only on the length of the shortest error event.

B. TC-MDPSK

Here, for any signalling period, the preceding signal provides the channel estimate; that is, $\hat{\alpha}_k = y_{k-1}$. Hence, the channel estimate has a variance of $b_1 = b_0 + \sigma^2$ and it can be shown that

$$|\mu|^2 = \frac{b_0 \rho^2(T_s)}{b_0 + 0.5\gamma_s^{-1}} = \frac{b_0 \delta}{b_0 + 0.5\gamma_s^{-1}} \quad (16)$$

where $\rho(\cdot)$ is the normalized autocorrelation function for a 3-rd order Butterworth spectrum, and $\delta \triangleq \rho^2(T_s)$. The above can be substituted in Eq. (11) to get the PEP. An examination of (16) reveals two facts. First, for very slow fading (i.e., $\rho(T_s) \approx 1$), at large signal-to-noise ratios μ approaches unity. Hence, the quality of the channel estimates is ideal. Second, for fast fading ($\rho(T_s) < 1$), no matter how large the signal-to-noise ratio, μ remains less than unity. This implies, for $\gamma_s \rightarrow \infty$, a fixed bit error probability, which is usually termed as an "error floor."

C. TC-MPSK WITH A PILOT TONE

As an alternative to differential detection, the α_k 's may be measured using some technique such as a pilot tone [5] or embedded pilot symbols [7]. If a reference tone is transmitted along with the data signal (both within the coherence bandwidth of the fading process), and if this tone can be filtered ideally, the resulting system performance will be almost equal to that of ideal coherent detection. Here, we assume these conditions.

For our purpose, we simply need to determine how the pilot-tone estimate correlates with the true channel gain. As in [5], the estimate $\hat{\alpha}_k$ is obtained by a pilot tone extraction filter with bandwidth of at least $2f_d$. Now the fraction of the total power spent on the data signal and the pilot tone is $1/(1+r)$ and $r/(1+r)$, respectively, where $r = P^2 T_s$. As in [5], we assume $B_p = 2f_d$. It then follows that [4]

$$\text{var}(\hat{\alpha}_k) = b_1 = b_0 + 0.5(B_p T_s) \left(\frac{1+r}{r} \right) \gamma_s^{-1}, \quad (17)$$

$$|\mu|^2 = \frac{b_0}{b_0 + 0.5(B_p T_s) \left(\frac{1+r}{r} \right) \gamma_s^{-1}}$$

where γ_s now accounts for the total symbol energy spent on both the data and pilot-tone. We note here that as \bar{E}_s/N_0 increases, the value of $|\mu|^2$ approaches unity. Thus, at large signal-to-noise ratios, the pilot tone technique is essentially equivalent to ideal coherent detection. The above can be substituted in Eq. (11) to get the PEP.

IV. RESULTS

A. THE UNION BOUND ON THE AVERAGE BIT ERROR RATE

Typically, the average bit error probability, a most important performance measure, can be bounded via the union

bound, which consists of infinitely many terms. Based on the PEP expressions developed here, all the terms may be enumerated using a transfer function. Then, the bit error probability of a TCM scheme with ideal interleaving/deinterleaving is upper bounded as

$$P_b \leq \frac{B(L_{\min})}{n} \frac{\partial T(D_1, D_2, \dots, I)}{\partial I} \Bigg|_{I=1} \quad (18)$$

where n is the number of input bits per encoding interval, and the D_i 's are the product terms in the approximations derived before, excluding $B(L)$, with each D_i being associated with d_i^2 . The transfer function $T(D_1, D_2, \dots, I)$ is determined by a signal flow graph, using *weight profile* and *uniformity* property [8].

In this study, we use a rate 2/3, eight-state binary convolutional encoder (see [9, Fig. 7]) to confirm the accuracy of the approximations developed thus far. The reader is referred to [9] for more details regarding the derivation of modified state transition diagram, augmented branch labels, and the modified encoder transfer function for this code.

B. COMPUTER SIMULATIONS

The rate 2/3 8-state convolutional encoder with 8-PSK signal set was used to encode a random data stream (the code is taken from [9]). The receiver was implemented using the Viterbi algorithm, with the decoding metric given in (5). In the Viterbi decoder, a decision depth of 18 symbols was used, that is, 6 times the code memory [2].

For the three detection methods, simulation results and the upper bounds are depicted in Figs. 2-4. There is satisfactory agreement between error bounds and simulation results.

V. CONCLUSIONS

New error bounds for TCM schemes operating on the shadowed Rician fading channel have been derived, which can be readily used with the transfer function method to obtain an upper bound on the bit error probability. The application of the resulting bounds has been exemplified for a moderately complex eight-state TCM scheme transmitted through this channel. For bit error rates less than 1×10^{-3} , the derived error bounds are within about 0.5 dB of the simulation results. The results may be useful in evaluating the performance of TCM schemes over shadowed channels.

REFERENCES

- [1] P. J. McLane *et al.*, "PSK and DPSK trellis codes for fast fading, shadowed mobile satellite communication channels," *IEEE Trans. Commun.*, vol. 36, pp. 1242-1246, Nov. 1988.
- [2] P. J. McLane *et al.*, "PSK and DPSK trellis codes for fast fading, shadowed mobile satellite communication channels," in *Proc. 1987 Int. Conf. Commun.*, (Seattle, WA), pp. 726-731, June 1988.
- [3] A. C. M. Lee and P. J. McLane, "Convolutionally interleaved PSK and DPSK trellis code for shadowed, fast fading mobile satellite communication channels," *IEEE Trans. Veh. Technol.*, vol. 39, pp. 37-47, June 1990.

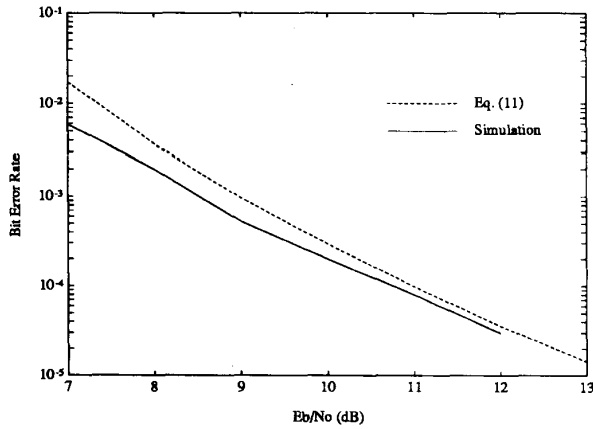


Figure 2: P_b versus \bar{E}_b/N_0 for coherent detection in light shadowed Rician.

- [4] C. Tellambura, Q. Wang and V. K. Bhargava, "A performance analysis of trellis-coded modulation schemes over Rician fading channels," to appear in *IEEE Trans. Veh. Technol.*, 1993.
- [5] J. K. Cavers and P. Ho, "Analysis of the error performance of trellis coded modulations in Rayleigh fading channels," *IEEE Trans. Commun.*, vol. 40, pp. 74-83, Jan. 1992.
- [6] J. Huang and L. Campbell, "Trellis coded MDPSK in correlated and shadowed Rician fading channels," *IEEE Trans. Veh. Technol.*, vol. 40, pp. 786-797, Nov. 1991.
- [7] J. K. Cavers, "An analysis of pilot symbol assisted modulation for Rayleigh fading channels," *IEEE Trans. Veh. Technol.*, vol. 40, pp. 686-693, Nov. 1991.
- [8] E. Biglieri and P. J. McLane, "Uniform distance and error probability properties of TCM schemes," *IEEE Trans. Commun.*, vol. 39, pp. 41-52, Jan. 1991.
- [9] R. G. McKay *et al.*, "Error bounds for trellis-coded MPSK on a fading mobile satellite channel," *IEEE Trans. Commun.*, vol. 39, pp. 1750-1761, Dec. 1991.

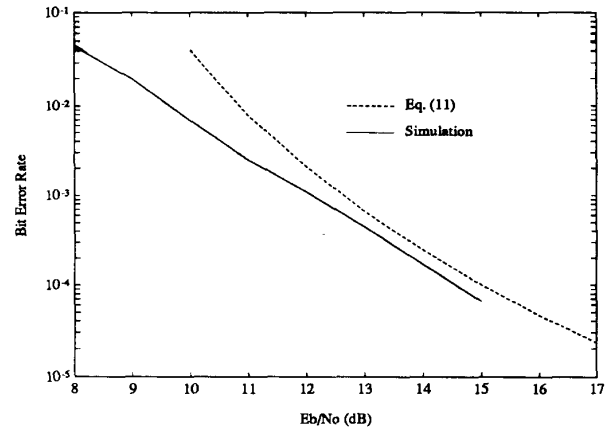


Figure 3: P_b versus \bar{E}_b/N_0 for differential detection in light shadowed Rician, $f_d T_s = 0.05$.

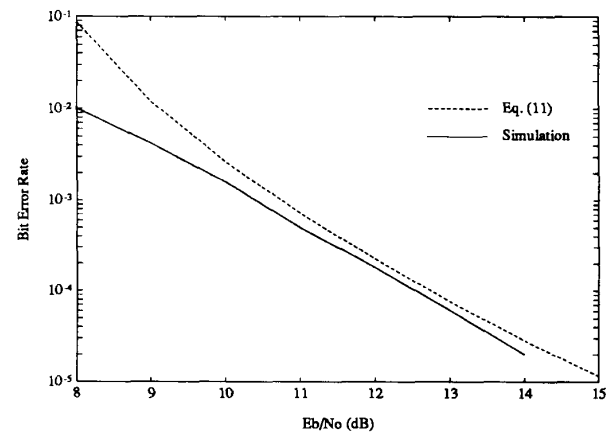


Figure 4: P_b versus \bar{E}_b/N_0 pilot-tone detection in light shadowed Rician, $f_d T_s = 0.05$.